

# Synchrosqueezing-based Recovery of Instantaneous Frequency from Nonuniform Samples

Gaurav Thakur\* and Hau-Tieng Wu†

June 24, 2011

## Abstract

We propose a new approach for studying the notion of the instantaneous frequency of a signal. We build on ideas from the Synchrosqueezing theory of Daubechies, Lu and Wu and consider a variant of Synchrosqueezing, based on the short-time Fourier transform, to precisely define the instantaneous frequencies of a multi-component AM-FM signal. We describe an algorithm to recover these instantaneous frequencies from the uniform or nonuniform samples of the signal and show that our method is robust to noise. We also consider an alternative approach based on the conventional, Hilbert transform-based notion of instantaneous frequency to compare to our new method. We use these methods on several test cases and apply our results to a signal analysis problem in electrocardiography.

Keywords: Instantaneous frequency, Synchrosqueezing, Nonuniform sampling, AM-FM signals, Electrocardiography

Mathematics Subject Classification (2010): 42C99, 42A38

## 1 Introduction

In a recent paper [5], Daubechies, Lu and Wu proposed and analyzed an adaptive wavelet-based signal analysis method that they called “Synchrosqueezing.” The authors considered continuous-domain signals that are a superposition of a finite number of approximately harmonic components, and they showed that Synchrosqueezing is able to decompose an arbitrary signal of this type. They showed that for such signals, Synchrosqueezing provides accurate instantaneous frequency information about their constituent components.

The concept of instantaneous frequency is a natural extension of the usual Fourier frequency that describes how fast a signal oscillates locally at a given point in time, or more generally, the different rates of oscillation at a given time. However, instantaneous frequency has so far remained a somewhat heuristic concept and has lacked a definition that is both mathematically rigorous and entirely satisfactory [11]. The analysis of signals from samples spaced nonuniformly in time is also an important problem in several applications, arising in radar detection, audio processing, seismology and many other fields [1, 12]. In this paper, we propose a new approach based on Synchrosqueezing to precisely define the instantaneous frequencies of a signal, and to recover these instantaneous frequencies from the uniform or nonuniform samples of the signal.

---

\*Program in Applied and Computational Mathematics, Princeton University, Princeton, NJ 08544, USA

†Mathematics Department, Princeton University, Princeton, NJ 08544, USA

We consider a class of multi-component AM-FM signals, comparable to the type studied in [5], and define a variant of Synchrosqueezing based on ideas similar to those in [5] but using the short-time Fourier transform (STFT). We show that by applying this modified Synchrosqueezing transform to an impulse train weighted by the samples, we can determine the instantaneous frequencies of the signal with high accuracy. We show furthermore that this procedure is robust with respect to noise. For purposes of comparison, we also consider a parallel approach based on the conventional, Hilbert transform-based notion of instantaneous frequency, combined with a well known least-squares method for bandlimited signal reconstruction from nonuniform samples [10]. We apply both methods to several test cases and compare their performance. We also consider a problem concerning the extraction of respiration data from a single-lead electrocardiogram (ECG) signal, and show how these methods can be used to study it.

This paper is organized as follows. In Section 2, we briefly review the conventional approach to instantaneous frequency. In Section 3, we describe our Synchrosqueezing-based algorithm and present the main new concepts and results of the paper. Our adaptation of the least-squares method for bandlimited functions is described in Section 4. We then perform our numerical experiments in Section 5 and discuss the application to ECG analysis.

## 2 Background Material

We first discuss the precise meaning of the instantaneous frequency (IF) of a signal and some of the obstacles encountered in computing it. We start by making a few definitions. Let  $f$  be a tempered distribution. We denote the forward and inverse Fourier transforms of  $f$  by  $\hat{f}$  and  $\check{f}$ , using the normalization  $\widehat{e^{-\pi x^2}} = e^{-\pi \xi^2}$ . For a fixed window function  $g$  in the Schwartz class  $\mathcal{S}$ , we denote the *modified short-time Fourier transform* of  $f$  by

$$V_g f(t, \eta) := \int_{-\infty}^{\infty} f(x) g(x-t) e^{-2\pi i \eta (x-t)} dx. \quad (1)$$

This is simply the regular STFT with a modulation factor  $e^{2\pi i \eta t}$ , which will be convenient for our purposes. We will also occasionally write  $f_1 \approx f_2$  if the inequality  $C_1 f_1 \leq f_2 \leq C_2 f_1$  holds, where  $C_1$  and  $C_2$  are constants independent of  $f_1$  and  $f_2$ . Finally, we will let  $\text{sinc}(x) := \frac{\sin(\pi x)}{\pi x}$ .

We now consider a function  $f$  having the AM-FM form  $f(t) = A(t) \cos(2\pi \phi(t))$ . We want to determine  $\phi'(t)$ , which intuitively describes the local rate of oscillation of  $f$  at  $t$ . This leads to the following general definition.

**Definition 2.1.** Suppose  $f$  is a superposition of  $K$  AM-FM components, having the form

$$f(t) = \sum_{k=1}^K A_k(t) \cos(2\pi \phi_k(t)) \quad (2)$$

with  $\phi'_k(t) > 0$  for all  $k$ . Then the *ideal instantaneous frequencies*  $\text{IIF}(f, A_k, \phi_k)$  are defined to be the set of functions  $\{\phi'_k(t)\}_{1 \leq k \leq K}$ .

Note that this concept only makes sense if all the component functions  $A_k$  and  $\phi_k$  are known, and it is impossible to define the IF of an arbitrary function  $f$  in this way. In fact, an arbitrary  $f$  will generally not have a unique representation of the form (2), with many different choices of  $A_k$ ,  $\phi_k$  and  $K$  possible. Even if we restrict  $K = 1$ , there is in general no way to separate the amplitude factor  $A_1$  from the frequency

factor  $\cos(2\pi\phi_1)$  without having some additional information on  $f$ .

In data analysis applications, we typically only know the full signal  $f$  and we want to obtain an approximation to the IIF. One of the most commonly used approaches for doing this can be described as follows [11]. For an appropriate  $f$ , we define the operator  $P^+f = (f + i\mathcal{H}f)/2$ , where  $\mathcal{H}f = (-i\text{sign}(\eta)\hat{f}(\eta))^\wedge$  is the Hilbert transform of  $f$ .  $P^+$  is known as the *Riesz projection* in mathematics and as the *single-sideband modulation* or the *analytic signal* in the engineering literature. We then consider the *Hilbert transform IIF* given by

$$\text{IF}_H f(t) = \frac{1}{2\pi} \text{Im} \left( \frac{\partial_t P^+ f(t)}{P^+ f(t)} \right). \quad (3)$$

The motivation for this concept is that the function  $f$  is assumed to have the form (2) with a single AM-FM component,  $f(t) = A(t) \cos(2\pi\phi(t))$ , and under some conditions,  $\text{IF}_H f(t)$  is a good approximation to  $\phi'(t)$ . The *Bedrosian theorem* states that if  $\text{supp}(\hat{A})$  and  $\text{supp}(\widehat{\cos(2\pi\phi)})$  are disjoint, then  $P^+ f(t) = A(t) \cdot P^+ \cos(2\pi\phi(t))$ . If we additionally assume that  $\text{supp}(\exp(2\pi i\phi)) \subset [0, \infty)$ , then  $P^+ \cos(2\pi\phi(t)) = e^{2\pi i\phi(t)}$ , and we have  $\text{IF}_H f(t) = \frac{1}{2\pi} \text{Im} \left( 2\pi i \phi'(t) + \frac{A'(t)}{A(t)} \right) = \phi'(t)$ .

These conditions on  $A$  and  $\phi$  are fairly restrictive and can be hard to verify for real-world signals, particularly the requirement that  $\text{supp}(\widehat{\exp(2\pi i\phi)}) \subset [0, \infty)$ . Even when they hold, the computation of  $\text{IF}_H$  is often sensitive to noise and numerical roundoff errors due to the Hilbert transform computation and the possible cancellation of zeros in the numerator and denominator of (3). In spite of this,  $\text{IF}_H$  has proven to give meaningful results for signals arising from a variety of applications, and is in widespread use in data analysis. We refer to the papers [11] and [3] for more details on the physical interpretation of  $\text{IF}_H$ . In Section 3, we will propose an alternative approach based on different ideas to approximate the IIF of a signal. We return to  $\text{IF}_H$  in Section 4 and show how it can be computed from nonuniform samples of a bandlimited signal.

### 3 Synchrosqueezing with the Short-Time Fourier Transform

Synchrosqueezing is an approach originally introduced in the context of audio signal analysis in [6] and was recently developed further in [5]. Synchrosqueezing belongs to the family of time-frequency reassignment methods and is a nonlinear operator that “sharpens” the time-frequency plot of a signal’s continuous wavelet transform so that it provides more useful information about the IF. In contrast to the reassignment methods discussed in [2], Synchrosqueezing is highly adaptive to the given signal and largely independent of the particular wavelet used, and also allows the signal to be reconstructed from the reassigned wavelet coefficients. We refer to the paper [5] for more details.

In this paper, we take a slightly different approach to Synchrosqueezing than in [5], based on the modified short-time Fourier transform. We will develop our theory independently of the results in [5] and show that this new Synchrosqueezing transform provides a way to estimate the IIF of a given function from discrete, nonuniform samples of the function. We will make a series of definitions leading up to our main theorem. We first define the following class of functions.

**Definition 3.1. (Intrinsic Mode Functions)**

The space  $\mathcal{B}_\epsilon$  of *Intrinsic Mode Functions (IMFs) of type B* consists of functions  $f$  having the form

$$f(t) = A(t)e^{2\pi i\phi(t)} \quad (4)$$

such that for some fixed  $\epsilon \ll 1$ ,  $A$  and  $\phi$  satisfy the following conditions:

$A, \phi \in L^\infty \cap C^\infty$ ,  $A^{(m)}, \phi^{(m)} \in L^\infty$  for all  $m$ ,  $A(t) > 0$ ,  $\phi'(t) > 0$ ,

$$\|A'\|_{L^\infty} \leq \epsilon \|\phi'\|_{L^\infty}, \quad \|\phi''\|_{L^\infty} \leq \epsilon \|\phi'\|_{L^\infty}.$$

We then consider the function class  $\mathcal{B}_{\epsilon,d}$ , defined as follows.

**Definition 3.2. (Superpositions of IMFs)**

The space  $\mathcal{B}_{\epsilon,d}$  of *superpositions of IMFs* consists of functions  $f$  having the form

$$f(t) = \sum_{k=1}^K f_k(t)$$

for some  $K > 0$  and  $f_k = A_k e^{2\pi i \phi_k} \in \mathcal{B}_\epsilon$  such that the  $\phi_k$  satisfy

$$\inf_t \phi'_k(t) - \sup_t \phi'_{k-1}(t) > d.$$

Our main results in this paper will be stated for  $\mathcal{B}_{\epsilon,d}$  functions. Intuitively, functions in  $\mathcal{B}_{\epsilon,d}$  are composed of several oscillatory components with slowly time-varying amplitudes and IIFs (we call these components IMFs, following [5]), and the IIFs of any two consecutive components are separated by at least  $d$ . This function class is fairly restrictive, but it turns out to be a reasonable model of signals that arise in many applications, and the conditions on the IMFs will allow us to obtain accurate estimates of the IIF of  $f$ . Note, however, that  $\mathcal{B}_{\epsilon,d}$  is not a vector space. We next define a closely related notion.

**Definition 3.3. (Impulse Trains)**

Let  $T > 0$  and  $\{a_n\} \in l^\infty$  with  $\|\{a_n\}\|_{l^\infty} \leq T^2$ . The *impulse train class* is defined by

$$\mathcal{D}_{\epsilon,d}^{T,\{a_n\}} = \left\{ \sum_{n=-\infty}^{\infty} (T + a_{n+1} - a_n) \delta(t - Tn - a_n) f(t) : f \in \mathcal{B}_{\epsilon,d} \right\}.$$

We can treat elements of the impulse train class  $\mathcal{D}_{\epsilon,d}^{T,\{a_n\}}$  as tempered distributions. As  $T \rightarrow 0$ ,  $\tilde{f} \in \mathcal{D}_{\epsilon,d}^{T,\{a_n\}}$  converges weakly to  $f \in \mathcal{B}_{\epsilon,d}$  with respect to Schwartz test functions, so  $\mathcal{D}_{\epsilon,d}^{T,\{a_n\}}$  can be thought of as a sampled version of the continuous-domain  $\mathcal{B}_{\epsilon,d}$  class. In applications, we are given a collection of nonuniformly spaced samples of the form  $\{f(t_n)\}$ ,  $t_n = Tn + a_n$ , where  $\{a_n\}$  represents a small perturbation from uniform samples  $\{Tn\}$  with sampling interval  $T$ . This can be converted to an element in the class  $\mathcal{D}_{\epsilon,d}^{T,\{a_n\}}$  by multiplying  $f(t_n)$  by a factor  $t_{n+1} - t_n = T + a_{n+1} - a_n$ .

For a given window function  $g \in \mathcal{S}$ , we can apply the modified short-time Fourier transform (1) to any  $\tilde{f} \in \mathcal{D}_{\epsilon,d}^{T,\{a_n\}}$ , with the tempered distribution  $\tilde{f}$  acting on  $g(\cdot - t)e^{-2\pi i \eta(\cdot - t)} \in \mathcal{S}$ . When  $|V_g \tilde{f}(t, \eta)| > 0$ , we define the *instantaneous frequency information*  $\omega \tilde{f}(t, \eta)$  by

$$\omega \tilde{f}(t, \eta) = \frac{\partial_t V_g \tilde{f}(t, \eta)}{2\pi i V_g \tilde{f}(t, \eta)}. \quad (5)$$

The idea with (5) is that  $\partial_t V_g \tilde{f}$  is a first approximation to the IF of  $f$ , and dividing by  $V_g \tilde{f}$  “removes the influence” of the window  $g$  and sharpens the resulting time-frequency plot. We can use this to consider the following operator, which will be our main computational tool in this paper.

**Definition 3.4. (STFT Synchrosqueezing)**

For  $\tilde{f} \in \mathcal{D}_{\epsilon,d}^{T,\{a_n\}}$ , the *STFT Synchrosqueezing transform with resolution  $\alpha > 0$  and threshold  $\gamma \geq 0$*  is defined by

$$S^{\alpha,\gamma}\tilde{f}(t,\xi) = \left| \left\{ \eta : |\xi - \omega\tilde{f}(t,\eta)| < \frac{\alpha}{2}, |V_g\tilde{f}(t,\eta)| \geq \gamma, 0 \leq \eta \leq \frac{1}{T} \right\} \right| \quad (6)$$

where  $(t,\xi) \in \mathbb{R} \times \alpha\mathbb{N}$  and  $|\cdot|$  denotes the Lebesgue measure on  $\mathbb{R}$ .

$S^{\alpha,\gamma}\tilde{f}$  is a kind of highly concentrated version of  $\omega\tilde{f}$  that “squeezes” the content of  $\omega\tilde{f}$  closer to the IF curves in the time–frequency plane. We are finally in a position to define an alternative notion of instantaneous frequency, based on the concepts discussed above.

**Definition 3.5. (Synchrosqueezing-based Instantaneous Frequency)**

The *Synchrosqueezing-based IF with resolution  $\alpha$  and threshold  $\gamma$*  of  $f \in \mathcal{B}_{\epsilon,d}$ , estimated from a corresponding  $\tilde{f} \in \mathcal{D}_{\epsilon,d}^{T,\{a_n\}}$ , is a set-valued function  $\text{IF}_S f(t) : \mathbb{R} \rightarrow 2^{\alpha\mathbb{N}}$  given by

$$\text{IF}_S f(t) = \left\{ \alpha n : n \in \mathbb{N}, S^{\alpha,\gamma}\tilde{f}(t, \alpha n) > 0 \right\}.$$

As a motivating example of this concept, let  $f(t) = e^{2\pi it} \in \mathcal{B}_{\epsilon,d}$ . The IIF is clearly the singleton  $\{1\}$ . For the window  $g(t) = e^{-\pi t^2}$ , we can compute  $V_g f(t,\eta) = e^{2\pi it - \pi(\eta-1)^2}$ , so  $\omega(t,\eta) = 1$  for all  $(t,\eta)$ . This means that for  $\gamma = 0$ ,  $S^{\alpha,\gamma}f(t,\xi)$  will be supported on  $\{[\frac{1}{\alpha}]\alpha, \lceil \frac{1}{\alpha} \rceil \alpha\}$  for all  $t$ , which is close to  $\{1\}$  for small  $\alpha$ . We will show in Theorem 3.6 that if  $\tilde{f} \in \mathcal{D}_{\epsilon,d}^{T,\{a_n\}}$  is a sampled approximation of  $f$  and  $\alpha$  and  $\gamma$  are chosen appropriately, then it has the same  $\text{IF}_S$  set.

We will use several auxiliary notations in the statement and proof of our main theorem. Let

$$\tilde{f}(t) = \sum_{k=1}^K \sum_{n=-\infty}^{\infty} \delta(t - Tn - a_n)(T + a_{n+1} - a_n)A_k(t)e^{2\pi i\phi_k(t)} \in \mathcal{D}_{\epsilon,d}^{T,\{a_n\}}. \quad (7)$$

We then define the following expressions:

$$\begin{aligned} I_n^{(m)} &:= \int_{-\infty}^{\infty} |u|^n |g^{(m)}(u)| du \\ \mathcal{I} &:= \bigcup_{n \in \mathbb{Z}} \mathcal{I}_n, \quad \mathcal{I}_n = [Tn, Tn + a_n] \text{ if } a_n \geq 0 \text{ or } [Tn + a_n, Tn] \text{ if } a_n < 0 \\ E_1 &:= \sum_{k=1}^K \epsilon \|\phi'_k\|_{L^\infty} (I_1 + \pi \|A_k\|_{L^\infty} I_2) \\ E'_1 &:= \sum_{k=1}^K \epsilon \|\phi'_k\|_{L^\infty} \left( \frac{1}{2\pi} I_0 + (\|A_k\|_{L^\infty} + \|\phi'_k\|_{L^\infty}) I_1 + \pi \|A_k\|_{L^\infty} \|\phi'_k\|_{L^\infty} I_2 \right) \\ E_3 &:= \sup_{1 \leq k \leq K} \|\phi'_k\|_{L^\infty} \end{aligned}$$

This leads to the following results.

**Theorem 3.6.** Let  $0 \leq T \leq 1$ . Suppose we have  $\tilde{f} \in \mathcal{D}_{\epsilon,d}^{T,\{a_n\}}$  as in (7) with  $\|\{a_n\}\|_{l^\infty} \leq T^2$ , and a window function  $g \in \mathcal{S}$  with  $\text{supp}(\hat{g}) \subset [-\frac{d}{2}, \frac{d}{2}]$  and  $\int_{\mathcal{I}} |g(x)| + |g'(x)| dx \leq \frac{\kappa}{T} \|\{a_n\}\|_{l^\infty}$  for a constant  $\kappa$ . Then there exist numbers  $E_2 = E_2(A_k, \phi_k, g)$  and  $E'_2 = E'_2(A_k, \phi_k, g)$  such that if we have a given resolution  $\alpha$  satisfying

$$\alpha \geq \frac{2(E'_1 + E'_2)}{E_1 + E_2} + 2E_3,$$

then the following statements hold.

1. Let  $0 \leq \eta \leq \frac{1}{T}$  and fix  $k$ ,  $1 \leq k \leq K$ . For each pair  $(t, \eta) \in Z_k := \{(t, \eta) : |\eta - \phi'_k(t)| < \frac{d}{2}\}$  with  $|V_g \tilde{f}(t, \eta)| > E_1 + E_2$ , we have  $|\omega \tilde{f}(t, \eta) - \phi'_k(t)| < \frac{\alpha}{2}$ . If  $(t, \eta) \notin Z_k$  for any  $k$ , then  $|V_g \tilde{f}(t, \eta)| \leq E_1 + E_2$ .
2. Suppose we have a threshold  $\gamma$  such that  $E_1 + E_2 < \gamma \leq |V_g \tilde{f}(t, \eta)|$  for all  $(t, \eta) \in Z_k$ . Then for all  $t$ ,  $S^{\alpha, \gamma} \tilde{f}(t, \xi)$  is supported in the  $2K$ -point set  $\bigcup_{1 \leq k \leq K} \{ \lfloor \frac{\phi'_k(t)}{\alpha} \rfloor \alpha, \lceil \frac{\phi'_k(t)}{\alpha} \rceil \alpha \}$ .

Theorem 3.6 says that the  $\text{IF}_S$  defined by STFT Synchrosqueezing approximates the IIF set accurately up to the preassigned resolution  $\alpha$ , without knowing anything about the symbolic form of  $f$ . The result also does not depend on the precise shape of the window  $g$  that we use, so the  $\text{IF}_S$  is in a sense adaptive to the structure of the sampled function  $\tilde{f}$ . The procedure suggested by Theorem 3.6 can be implemented as follows. We first discretize  $\tilde{f}$  on a uniform grid (finer than  $T$ ) by zero-padding in between the impulses. For each  $t$ , we can then compute  $V_g \tilde{f}$  and  $\partial_t V_g \tilde{f} = -V_{g'} \tilde{f} + 2\pi i \eta V_g \tilde{f}$  on using FFTs and use the results to approximate  $S^{\alpha, \gamma} \tilde{f}(t, \alpha n)$  for  $n \in \mathbb{N}$ . In practice, the upper bound on  $\eta$  in (6) is determined by how finely  $\tilde{f}$  is discretized, and as long as the threshold  $\gamma$  is not too small, we ignore the locations where the denominator in (5) is close to zero and avoid numerical stability issues. We finally find the (numerical) support of  $S^{\alpha, \gamma} \tilde{f}(t, \cdot)$  to determine the component(s) of  $\text{IF}_S f(t)$ .

There is a tradeoff between  $\alpha$  and  $\gamma$  and the fluctuation of the IIF components, and this is a kind of uncertainty principle that is inherent to the  $\text{IF}_S$  concept. The  $\text{IF}_S$  is only meaningful up to the resolution  $\alpha$ , and beyond that, we cannot approximate the IIF to any further level of accuracy. In the simplest case when the amplitudes  $\{A_k\}$  and IIF components  $\{\phi'_k\}$  are all constant, the lower bound on  $\alpha$  will be small and will allow us to specify a fine resolution  $\alpha$ , resulting in a very accurate estimate of the IIF. On the other hand, if the  $\{A'_k\}$  or  $\{\phi''_k\}$  are large, then the lower bound on  $\gamma$  will be significant, making  $S^{\alpha, \gamma} \tilde{f}(t, \xi) = 0$  for most  $t$ . In physical terms, the existence of a  $\gamma$  in Theorem 3.6 ensures that the magnitude of each component is not too small and its IIF is not too rapidly oscillating, or else the component would be indistinguishable from noise.

The proof of Theorem 3.6 involves a series of estimates. Let  $f$  and  $\tilde{f}$  be given as in Theorem 3.6. In what follows, we let  $Q_k(t, \eta) = A_k(t) e^{2\pi i \phi_k(t)} \hat{g}(\eta - \phi'_k(t))$  to simplify some notation.

**Lemma 3.7.** If  $(t, \eta) \in Z_k$  for some fixed  $k$ ,  $1 \leq k \leq K$ , then

$$|V_g f(t, \eta) - Q_k(t, \eta)| \leq E_1 \tag{8}$$

and

$$\left| \frac{1}{2\pi i} \partial_t V_g f(t, \eta) - \phi'_k(t) Q_k(t, \eta) \right| \leq E'_1. \tag{9}$$

If  $(t, \eta) \notin Z_k$  for any  $k$ , then

$$|V_g f(t, \eta)| \leq E_1 \quad \text{and} \quad \left| \frac{1}{2\pi i} \partial_t V_g f(t, \eta) \right| \leq E'_1.$$

*Proof.* Note that for any  $l$ , the bandwidth condition on  $g$  shows that  $Q_l(t, \eta) = 0$  whenever  $(t, \eta) \notin Z_l$ . We assume  $(t, \eta) \in Z_k$  for some  $k$ , as the other case can be done in exactly the same way. For the first bound (8), Taylor expansions show that

$$|1 - e^{2\pi i(-\phi_k(x) + \phi_k(t) + (x-t)\phi'_k(t))}| \leq \pi \|\phi''_k\|_{L^\infty} |x - t|^2.$$

It follows that

$$|V_g f(t, \eta) - Q_k(t, \eta)|$$

$$\begin{aligned}
&= \left| V_g f(t, \eta) - \sum_{k=1}^K Q_k(t, \eta) \right| \\
&\leq \sum_{k=1}^K \left[ \int_{-\infty}^{\infty} |A_k(x) - A_k(t)| |g(x-t)e^{-2\pi i \eta(x-t)}| dx \right. \\
&\quad \left. + |A_k(t)| \int_{-\infty}^{\infty} \left| e^{2\pi i \phi_k(x)} - e^{2\pi i(\phi_k(t) + (x-t)\phi'_k(t))} \right| |g(x-t)e^{-2\pi i \eta(x-t)}| dx \right] \\
&\leq \sum_{k=1}^K \left( \int_{-\infty}^{\infty} \|A'_k\|_{L^\infty} |x-t| |g(x-t)| dx + |A_k(t)| \int_{-\infty}^{\infty} \pi \|\phi''_k\|_{L^\infty} |x-t|^2 |g(x-t)| dx \right) \\
&\leq \sum_{k=1}^K \epsilon \|\phi'_k\|_{L^\infty} (I_1 + \pi \|A_k\|_{L^\infty} I_2).
\end{aligned}$$

We follow similar arguments for the second bound (9). We first have the estimate

$$\begin{aligned}
&|A_k(x)\phi'_k(x)e^{2\pi i \phi_k(x)} - A_k(t)\phi'_k(t)e^{2\pi i(\phi_k(t) + \phi'_k(t)(x-t))}| \\
&\leq |A_k(x)\phi'_k(x) - A_k(t)\phi'_k(t)| + |1 - e^{2\pi i(-\phi_k(x) + \phi_k(t) + \phi'_k(t)(x-t))}| |A_k(t)\phi'_k(t)| \\
&\leq (\|A_k\|_{L^\infty} \|\phi''_k\|_{L^\infty} + \|A'_k\|_{L^\infty} \|\phi'_k\|_{L^\infty}) |x-t| + \pi \|A_k\|_{L^\infty} \|\phi'_k\|_{L^\infty} \|\phi''_k\|_{L^\infty} |x-t|^2.
\end{aligned}$$

Thus we obtain

$$\begin{aligned}
&\left| \frac{1}{2\pi i} \partial_t V_g f(t, \eta) - \phi'_k(t) Q_k(t, \eta) \right| \\
&= \left| \sum_{k=1}^K \left[ -\frac{1}{2\pi i} \int_{-\infty}^{\infty} A_k(x) e^{2\pi i \phi_k(x)} \partial_x (g(x-t)e^{-2\pi i \eta(x-t)}) dx \right. \right. \\
&\quad \left. \left. - \phi'_k(t) A_k(t) \int_{-\infty}^{\infty} e^{2\pi i(\phi_k(t) + \phi'_k(t)(x-t))} g(x-t) e^{-2\pi i \eta(x-t)} dx \right] \right| \\
&\leq \sum_{k=1}^K \left[ \int_{-\infty}^{\infty} |A_k(x)\phi'_k(x)e^{2\pi i \phi_k(x)} - A_k(t)\phi'_k(t)e^{2\pi i(\phi_k(t) + \phi'_k(t)(x-t))}| |g(x-t)| dx \right. \\
&\quad \left. + \frac{1}{2\pi} \int_{-\infty}^{\infty} |A'_k(x)| |g(x-t)| dx \right] \\
&\leq \sum_{k=1}^K \epsilon \|\phi'_k\|_{L^\infty} \left( \|A_k\|_{L^\infty} I_1 + \|\phi'_k\|_{L^\infty} I_1 + \pi \|A_k\|_{L^\infty} \|\phi'_k\|_{L^\infty} I_2 + \frac{1}{2\pi} I_0 \right).
\end{aligned}$$

□

**Lemma 3.8.** Let  $0 \leq \eta \leq \frac{1}{T}$ . Then

$$|V_g \tilde{f}(t, \eta) - V_g f(t, \eta)| \leq E_2 \quad (10)$$

and

$$\frac{1}{2\pi} \left| \partial_t V_g \tilde{f}(t, \eta) - \partial_t V_g f(t, \eta) \right| \leq E'_2. \quad (11)$$

for some numbers  $E_2 = E_2(A_k, \phi_k, g)$  and  $E'_2 = E'_2(A_k, \phi_k, g)$  independent of  $\eta$  or  $T$ .

*Proof.* Suppose  $h \in C^1$ . Then denoting  $t_n = Tn + a_n$ , we have

$$\begin{aligned}
& \left| \sum_{n=-\infty}^{\infty} (t_{n+1} - t_n)h(t_n) - \int_{-\infty}^{\infty} h(t)dt \right| \\
&= \left| \sum_{n=-\infty}^{\infty} \int_{t_n}^{t_{n+1}} h'(u)(u - t_{n+1})du \right|. \\
&= \left| \int_{-\infty}^{\infty} h'(u) \sum_{n=-\infty}^{\infty} (u - t_{n+1})\chi_{[t_n, t_{n+1}]}(u)du \right|.
\end{aligned} \tag{12}$$

Since  $V_g \tilde{f}(t, \eta) = \sum_{n=-\infty}^{\infty} (t_{n+1} - t_n)f(t_n)g(t_n - t)e^{-2\pi i\eta(t_n - t)}$ , we use the above calculation to find that

$$\begin{aligned}
& \left| V_g \tilde{f}(t, \eta) - V_g f(t, \eta) \right| \\
&\leq \sum_{k=1}^K \left| \int_{-\infty}^{\infty} \partial_u \left( A_k(u)e^{2\pi i(\phi_k(u) - (u-t)\eta)} g(u-t) \right) \sum_{n=-\infty}^{\infty} (u - t_{n+1})\chi_{[t_n, t_{n+1}]}(u)du \right| \\
&\leq \sum_{k=1}^K \left( \left| \int_{-\infty}^{\infty} G(u)C(u)du \right| + 2\epsilon T \|\phi'_k\|_{L^\infty} I_0 + 2T \|A_k\|_{L^\infty} I'_0 \right),
\end{aligned} \tag{13}$$

where we let  $G(u) := 2\pi i A_k(u)(\phi'_k(u) - \eta)g(u-t)e^{2\pi i(\phi_k(u) - u\eta)}$  and  $C(u) := \sum_{n=-\infty}^{\infty} (u - t_{n+1})\chi_{[t_n, t_{n+1}]}(u)$ . For brevity, we will fix  $k$  and omit the subscripts on  $A_k$  and  $\phi_k$  in what follows. The function  $C(u)$  is well approximated by the uniform sawtooth function

$$W(u) = \sum_{n=-\infty}^{\infty} (u - T(n+1))\chi_{[Tn, T(n+1)]}(u) = - \sum_{n=1}^{\infty} \frac{\sin(2\pi n u/T)}{\pi n/T} - \frac{T}{2},$$

where the last equality holds for almost all  $u$ . We define the difference  $D(u) = W(u) - C(u)$ . Since  $G \in \mathcal{S}$ , using the Parseval theorem gives

$$\begin{aligned}
& \left| \int_{-\infty}^{\infty} G(u)C(u)du \right| \\
&= \left| - \int_{-\infty}^{\infty} G(u) \sum_{n=1}^{\infty} \frac{\sin(2\pi n u/T)}{\pi n/T} du - \hat{G}(0)\frac{T}{2} + \int_{-\infty}^{\infty} G(u)D(u)du \right| \\
&\leq \left| \sum_{n=1}^{\infty} \frac{T}{4\pi i n} \left( \hat{G}\left(\frac{2\pi n}{T}\right) - \hat{G}\left(-\frac{2\pi n}{T}\right) \right) \right| + \frac{T}{2} |\hat{G}(0)| + \left| \int_{-\infty}^{\infty} G(u)D(u)du \right|.
\end{aligned} \tag{14}$$

We now consider each term in (14) separately. For the first term, we will need an estimate of  $\hat{G}(\xi)$ . We claim that  $\hat{G}$  will be insignificant outside intervals centered at  $\phi'(u) - \eta$ . For any  $J > 0$ , let  $\xi$  be such that



$|\phi'(u) - \eta - \xi| \geq J$ . Then we have

$$\begin{aligned}
|\hat{G}(\xi)| &= 2\pi \left| \int_{-\infty}^{\infty} A(u)(\phi'(u) - \eta) e^{2\pi i(\phi(u) - (\eta + \xi)u)} g(u - t) du \right| \\
&= 2\pi \left| \int_{-\infty}^{\infty} e^{2\pi i(\phi(u) - (\eta + \xi)u)} \partial_u \left( \frac{A(u)(\phi'(u) - \eta)g(u - t)}{\phi'(u) - \eta - \xi} \right) du \right| \\
&\leq 2\pi \left( \frac{J(\epsilon \|A\|_{L^\infty} I_0 + \epsilon \|\phi'\|_{L^\infty} I_0 + \|\phi'\|_{L^\infty} \|A\|_{L^\infty} I'_0) + \epsilon \|\phi'\|_{L^\infty} \|A\|_{L^\infty} I_0}{J^2} \right. \\
&\quad \left. + \eta \frac{J(\epsilon I_0 + \|A\|_{L^\infty} I'_0) + \epsilon \|A\|_{L^\infty} I_0}{J^2} \right) \\
&\leq C_1(\eta + 1) \left( \frac{1}{J} + \frac{1}{J^2} \right), \tag{15}
\end{aligned}$$

where the constant  $C_1 = C_1(A_k, \phi_k, g)$  is independent of  $\eta$  or  $J$ . We take  $J = \max(\frac{2\pi n}{T} - L^+, L^- - \frac{2\pi n}{T}, \frac{\pi}{T})$  with the numbers  $L^+$  and  $L^-$  chosen such that  $L^- \leq |\phi'(u) - \eta| \leq L^+$  for all  $u$ . This gives

$$\begin{aligned}
&\left| \sum_{n=1}^{\infty} \frac{T}{4\pi i n} \left( \hat{G}\left(-\frac{2\pi n}{T}\right) - \hat{G}\left(\frac{2\pi n}{T}\right) \right) \right| \\
&\leq C_1(\eta + 1) \sum_{n=1}^{\infty} \frac{2T}{4\pi n \max(\frac{2\pi n}{T} - L^+, L^- - \frac{2\pi n}{T}, \frac{\pi}{T})} \\
&\leq C_1(\eta + 1) \sum_{n=1}^{\infty} 2 \max(|L^+ - L^-|, 1) \left( \frac{T}{2\pi n} \right)^2 \\
&= C_1 \max(|L^+ - L^-|, 1) \frac{T^2(\eta + 1)}{12}. \tag{16}
\end{aligned}$$

For the second term in (14), we consider two cases. If  $|\phi'(u) - \eta| \geq J$ , then calculations similar to those in (15) show that

$$\begin{aligned}
|\hat{G}(0)| &= 2\pi \left| \int_{-\infty}^{\infty} e^{2\pi i(\phi(u) - \eta u)} \partial_u \left( \frac{A'(u)g(u - t) + A(u)g'(u - t)}{\phi'(u) - \eta} \right) du \right| \\
&\leq 2\pi \left( \frac{\|A''\|_{L^\infty} I_0 + 2\|A'\|_{L^\infty} I'_0 + \|A\|_{L^\infty} I''_0}{J} + \frac{\|\phi'\|_{L^\infty} \|A'\|_{L^\infty} I_0 + \|\phi'\|_{L^\infty} \|A\|_{L^\infty} I'_0}{J^2} \right) \\
&\leq C_2 \left( \frac{1}{J} + \frac{1}{J^2} \right)
\end{aligned}$$

for some constant  $C_2$ . On the other hand, if  $|\phi'(u) - \eta| < J$ , then we can easily estimate  $|\hat{G}(0)| \leq \|G\|_{L^1} \leq 2\pi \|A\|_{L^\infty} J I_0$ . We now choose a  $J$  that minimizes  $\max(C_2 (\frac{1}{J} + \frac{1}{J^2}), 2\pi \|A\|_{L^\infty} J I_0)$  over all  $0 \leq \eta \leq \frac{1}{T}$ . This results in a bound of the form

$$\frac{T}{2} |\hat{G}(0)| \leq C_3 T \tag{17}$$

for a constant  $C_3$ . The third term in (14) is controlled by the nonuniform perturbation  $\{a_n\}$ . Note that if  $u \notin \mathcal{I}$ , then  $|D(u)| \leq 2 \|\{a_n\}\|_{l^\infty}$ , and for  $u \in \mathcal{I}$ , we have  $|D(u)| \leq T + 2 \|\{a_n\}\|_{l^\infty}$ . This gives

$$\begin{aligned}
& \left| \int_{-\infty}^{\infty} G(u)D(u)du \right| \\
&= \left| \int_{\mathcal{I}} G(u)D(u)du + \int_{\mathbb{R} \setminus \mathcal{I}} G(u)D(u)du \right| \\
&\leq \|\phi' - \eta\|_{L^\infty} \|A\|_{L^\infty} \left( (T + \|\{a_n\}\|_{l^\infty}) \int_{\mathcal{I}} |g(u)|du + I_0 \|\{a_n\}\|_{l^\infty} \right) \\
&\leq (\|\phi'\|_{L^\infty} + \eta) \|A\|_{L^\infty} ((T + T^2)\kappa T + I_0 T^2). \tag{18}
\end{aligned}$$

Combining (13), (16), (17) and (18), we end up with an estimate of the form

$$|V_g \tilde{f}(t, \eta) - V_g f(t, \eta)| \leq C_4(T + T^2(\eta + 1)),$$

for some  $C_4 = C_4(A_k, \phi_k, g)$  independent of  $T$ ,  $\{a_n\}$  or  $\eta$ . This finally implies the result (10). For the derivative inequality (11), we can simply use the result of (10) with  $g$  replaced by  $g'$ , which shows that for some  $C_5$ ,

$$\begin{aligned}
& \frac{1}{2\pi} \left| \partial_t V_g \tilde{f}(t, \eta) - \partial_t V_g f(t, \eta) \right| \\
&\leq \eta \sum_{k=1}^K \left( \left| \int_{-\infty}^{\infty} \partial_u (A_k(u)g(u-t)) e^{2\pi i(\phi_k(u)-\eta(u-t))} C(u) du \right| + \right. \\
&\quad \left. \frac{1}{2\pi} \left| \int_{-\infty}^{\infty} \partial_u (A_k(u)g'(u-t)) e^{2\pi i(\phi_k(u)-\eta(u-t))} C(u) du \right| \right) \\
&\leq C_5(T\eta + T^2\eta^2 + T^2\eta).
\end{aligned}$$

□

*Proof of Theorem 3.6.* For the first part of Theorem 3.6, we suppose that  $(t, \eta) \in Z_k$  for some  $k$ ,  $|V_g \tilde{f}(t, \eta)| > E_1 + E_2$  and  $0 \leq \eta \leq \frac{1}{T}$ . Putting Lemmas 3.7 and 3.8 together, we get  $|V_g \tilde{f}(t, \eta) - Q_k(t, \eta)| \leq E_1 + E_2$  and  $|\frac{1}{2\pi i} \partial_t V_g \tilde{f}(t, \eta) - \phi'_k(t) Q_k(t, \eta)| \leq E'_1 + E'_2$ . We conclude that

$$\begin{aligned}
& |\omega \tilde{f}(t, \eta) - \phi'_k(t)| \\
&= \left| \frac{\frac{1}{2\pi i} \partial_t V_g \tilde{f}(t, \eta) - \phi'_k(t) Q_k(t, \eta)}{V_g \tilde{f}(t, \eta)} + \frac{\phi'_k(t)(Q_k(t, \eta) - V_g \tilde{f}(t, \eta))}{V_g \tilde{f}(t, \eta)} \right| \\
&< \frac{E'_1 + E'_2 + E_3(E_1 + E_2)}{E_1 + E_2} \\
&\leq \frac{\alpha}{2}. \tag{19}
\end{aligned}$$

For the second part of the theorem, let  $t$  be fixed and suppose  $\xi \in \alpha\mathbb{N}$ ,  $\xi \notin \bigcup_{1 \leq k \leq K} \{ \lfloor \frac{\phi'_k(t)}{\alpha} \rfloor \alpha, \lceil \frac{\phi'_k(t)}{\alpha} \rceil \alpha \}$ . If  $(t, \eta) \notin Z_k$  for any  $k$ , then by Lemmas 3.7 and 3.8 we would have  $|V_g \tilde{f}(t, \eta)| \leq E_1 + E_2 < \gamma$ . But since  $|V_g \tilde{f}(t, \eta)| \geq \gamma$  by assumption,  $(t, \eta) \in Z_k$  for some  $k$ . If  $\xi > \lceil \frac{\phi'_k(t)}{\alpha} \rceil \alpha$ , then the estimate (19) gives

$$|\xi - \omega \tilde{f}(t, \eta)| \geq \xi - |\omega \tilde{f}(t, \eta)| \geq \xi - \phi'_k(t) - \frac{\alpha}{2} \geq \frac{\alpha}{2},$$

and similarly, if  $\xi < \lfloor \frac{\phi'_k(t)}{\alpha} \rfloor \alpha$ , we get  $|\xi - \omega \tilde{f}(t, \eta)| \geq |\omega \tilde{f}(t, \eta)| - \xi \geq \frac{\alpha}{2}$ . This means that  $\{\eta : |\xi - \omega \tilde{f}(t, \eta)| < \frac{\alpha}{2}, |V_g \tilde{f}(t, \eta)| \geq \gamma, 0 \leq \eta \leq \frac{1}{T}\} = \emptyset$  and so  $S^{\alpha, \gamma} \tilde{f}(t, \xi) = 0$ .  $\square$

*Remark.* We have studied functions  $f \in \mathcal{B}_{\epsilon, d}$  on the entire real line here, but we can instead consider such functions supported only on a finite interval, and the same results will hold with largely only notational changes. We can also consider real-valued functions  $f$  that have the exponentials  $e^{2\pi i \phi_k(t)}$  in (4) replaced by  $\cos(2\pi \phi_k(t))$ , and similar results will hold. The assumption that  $T \leq 1$  in Theorem 3.6 was made for convenience in the proof, but it poses no loss of generality since lower sampling rates are equivalent to simply rescaling  $f$  (and thus also its IIF).

*Remark.* In Theorem 3.6, we required the window  $g$  to be bandlimited to  $[-\frac{d}{2}, \frac{d}{2}]$ . This assumption is not strictly necessary and was made here to simplify the presentation. In general, it is enough for  $g \in \mathcal{S}$  to be such that  $|\hat{g}|$  is small outside  $[-\frac{d}{2}, \frac{d}{2}]$ . The Gaussian window  $g(t) = e^{-\pi t^2 d^2/4}$  works well in practice. For such a window, there will be an extra term in the error estimates in Lemma 3.7, but the results still remain essentially the same. (e.g. if we assume  $\|\hat{g}\|_{L^\infty(\mathbb{R} \setminus [-\frac{d}{2}, \frac{d}{2}])} \leq \epsilon$ , then instead of having  $Q_l(t, \eta) = 0$  for  $(t, \eta) \notin Z_l$ , we would get  $|Q_l(t, \eta)| \leq C\epsilon$  for a constant  $C$ .)

We finally show that if  $\alpha$  and  $\gamma$  are chosen properly, the calculation of  $\text{IF}_S$  is robust to sample noise. The argument is almost the same as in the proof of Theorem 3.6.

**Theorem 3.9.** Let  $0 \leq T \leq 1$ . Suppose  $\tilde{f} \in \mathcal{D}_{\epsilon, d}^{T, \{a_n\}}$  is as in (7) and let  $g$  be a window with the same conditions as in Theorem 3.6. Assume that the samples  $\{f(t_n)\} = \{f(Tn + a_n)\}$  are contaminated by noise  $\{N_n\}$  with  $\|\{N_n\}\|_{l^\infty} \leq T$ , i.e. we are given  $\bar{f} = \tilde{f} + \sum_{n=-\infty}^{\infty} (t_{n+1} - t_n) \delta(\cdot - t_n) N_n$ . Suppose we have a resolution  $\alpha$  satisfying

$$\alpha \geq \frac{2(E'_1 + E'_2 + I_0 + 2I'_0 + \frac{1}{2\pi}(I'_0 + 2I''_0))}{E_1 + E_2 + I_0 + 2I'_0} + 2E_3,$$

where  $E_2$  and  $E'_2$  are as in Lemma 3.8. Then the following statements hold.

1. Let  $0 \leq \eta \leq \frac{1}{T}$  and fix  $k$ ,  $1 \leq k \leq K$ . For each pair  $(t, \eta) \in Z_k$  with  $|V_g \bar{f}(t, \eta)| > E_1 + E_2 + I_0 + 2I'_0$ , we have  $|\omega \bar{f}(t, \eta) - \phi'_k(t)| < \frac{\alpha}{2}$ . If  $(t, \eta) \notin Z_k$  for any  $k$ , then  $|V_g \bar{f}(t, \eta)| \leq E_1 + E_2 + I_0 + 2I'_0$ .
2. Suppose we have a threshold  $\gamma$  such that  $E_1 + E_2 + I_0 + 2I'_0 < \gamma \leq |V_g \bar{f}(t, \eta)|$  for all  $(t, \eta) \in Z_k$ . Then for all  $t$ ,  $S^{\alpha, \gamma} \bar{f}(t, \xi)$  is supported in the  $2K$ -point set  $\bigcup_{1 \leq k \leq K} \{\lfloor \frac{\phi'_k(t)}{\alpha} \rfloor \alpha, \lceil \frac{\phi'_k(t)}{\alpha} \rceil \alpha\}$ .

The only part of the proof different from Theorem 3.6 is the estimate in Lemma 3.8, which we replace by the following inequalities.

**Lemma 3.10.** Let  $0 \leq \eta \leq \frac{1}{T}$ . Then

$$|V_g \bar{f}(t, \eta) - V_g f(t, \eta)| \leq E_2 + I_0 + 2I'_0$$

and

$$\frac{1}{2\pi} |\partial_t V_g \bar{f}(t, \eta) - \partial_t V_g f(t, \eta)| \leq E'_2 + I_0 + 2I'_0 + \frac{1}{2\pi} (I'_0 + 2I''_0).$$

*Proof.* Lemma 3.8 and the inequality (12) imply that

$$\begin{aligned} & |V_g \bar{f}(t, \eta) - V_g f(t, \eta)| \\ & \leq |V_g \tilde{f}(t, \eta) - V_g f(t, \eta)| + \|N_n\|_{l^\infty} \sum_{n=-\infty}^{\infty} |(t_{n+1} - t_n) g(t_n - t)| \\ & \leq E_2 + T(I_0 + 2TI'_0), \end{aligned}$$

and similarly,

$$\frac{1}{2\pi} |\partial_t V_g \bar{f}(t, \eta) - \partial_t V_g f(t, \eta)| \leq E'_2 + \eta T(I_0 + 2TI'_0) + \frac{1}{2\pi} T(I'_0 + 2TI''_0).$$

□

Combining these bounds with the other estimates in the proof of Theorem 3.6 gives Theorem 3.9.

## 4 A Bandlimited Reconstruction Approach

We now consider a somewhat different formulation and approach towards our problem, based on the traditional  $\text{IF}_H$  concept. Suppose we have the samples  $\{f(t_k)\}$  of a function  $f \in L^2$  with  $\text{supp}(\hat{f}) \subset [-b, b]$ . We want to determine  $f$  and use it to find  $\text{IF}_H f$ . In the case of uniformly spaced samples, i.e.  $t_k = Tk$  for a constant  $T > 0$ , it is well known that  $f$  can be recovered if the sampling rate  $\frac{1}{T}$  exceeds  $2b$ , the Nyquist frequency of  $f$ . There are analogous results for very general classes of nonuniform sampling points  $\{t_k\}$  [1, 12]. As in Section 3, we will consider sampling points  $\{t_k\} = \{Tk + a_k\}$  that are small perturbations of uniformly spaced points. Suppose the sequence  $\{t_k\}$  is indexed so that  $t_k < t_{k+1}$  and that for some  $T > 0$ ,

$$\sup_k |t_k - Tk| < \frac{T}{2}. \quad (20)$$

If  $\frac{1}{T} > 2b$ , it can be shown that  $C_1 \|f\|_{L^2} \leq \|f(t_k)\|_{l^2} \leq C_2 \|f\|_{L^2}$ , where the constants  $C_1$  and  $C_2$  depend only on  $\{t_k\}$  and  $b$  [8, 10]. When the  $t_k$  are uniformly spaced, i.e.  $t_k = Tk$ , the Plancherel formula shows that  $C_1 = C_2 = T^{-1/2}$ . For the rest of this section, we assume that  $\{t_k\}$  satisfies (20) with  $\frac{1}{T} > 2b$ , which intuitively means that the sampling points  $\{t_k\}$  are evenly spread out over  $\mathbb{R}$  and have an ‘‘average’’ sampling rate above the Nyquist rate.

One of the standard approaches for recovering  $f$  from the samples  $f(t_k)$  involves solving the linear least-squares problem

$$\{\tilde{c}_{k,N}\} = \underset{\{c_k\} \in \mathbb{C}^{2N+1}}{\text{argmin}} \left\| w_k \left( f(t_k) - \sum_{n=-N}^N c_n h(n, t_k/T) \right) \right\|_{l^2}^2, \quad (21)$$

where  $\{h(n, t)\}_{n \in [-N, N]}$  is a given set of basis functions and the  $w_k$  are some weights such that  $|w_k| \approx 1$  for all  $k$  [10, 12, 9]. If the basis and weights are chosen appropriately, the function

$$f_N(t) = \sum_{n=-N}^N \tilde{c}_{n,N} h(n, t) \quad (22)$$

is a good approximation to  $f_T(t) := f(Tt)$ . There have been a couple of efficient algorithms developed around this idea, usually using the DFT basis  $h(n, t) = (2N + 1)^{-1/2} e^{-2\pi i n t / (2N+1)}$  and the weights  $w_k = \frac{t_{k+1} - t_{k-1}}{2}$ . For these choices, as  $N \rightarrow \infty$ ,  $f_N$  converges uniformly to  $f_T$  on compact subsets of  $\mathbb{R}$ , and the matrix computations used in solving the problem (21) are well-conditioned and can be accelerated using FFTs [10]. Once we have an expansion of the form (22), it follows by linearity that  $P^+ f_N(t) = \sum_{n=-N}^N \tilde{c}_{n,N} P^+ h(n, t)$ , and we can use this to find  $\text{IF}_H f$ .

We will prefer to use the basis  $h(n, t) = \text{sinc}(t - n - M)$  in this paper, where  $M$  is an integer constant, along with the same weights  $w_k$  as above. In this case,  $f_N$  converges to  $f_T$  uniformly on the entire real line, and we have found that in practice, this results in a better accuracy with the computation of

$P^+ f_N$ . This choice of  $h(n, t)$  can be justified by the following argument. For any vector  $\{c_k\} \in l^2$  with  $\text{supp}(c_k) \subset [M - N, M + N]$ , we have

$$\begin{aligned} \|f_T(k) - c_k\|_{l^2} &= \left\| f_T(t) - \sum_{n=-N}^N c_{n+M} \text{sinc}(t - n - M) \right\|_{L^2} \\ &\approx \left\| f(t_k) - \sum_{n=-N}^N c_{n+M} \text{sinc}(t_k/T - n - M) \right\|_{l^2} \\ &\approx \left\| w_k \left( f(t_k) - \sum_{n=-N}^N c_{n+M} \text{sinc}(t_k/T - n - M) \right) \right\|_{l^2}. \end{aligned}$$

By taking the minimum over  $\{c_k\}$ , it follows that for  $\{\tilde{c}_{k,N}\}$  given by (21),

$$\|f_T(k) - \tilde{c}_{k,N}\|_{l^2} \approx \|f_T(k) - f_T(k) \chi_{[M-N, M+N]}(k)\|_{l^2} \rightarrow 0$$

as  $N \rightarrow \infty$ . We can then conclude that

$$\|f_T - f_N\|_{L^\infty} \leq \|\hat{f}_T - \hat{f}_N\|_{L^1} \leq \|f_T - f_N\|_{L^2} = \|f_T(k) - \tilde{c}_{k,N}\|_{l^2} \rightarrow 0.$$

So we essentially determine uniform samples of  $f$  from the nonuniform samples  $\{f(t_k)\}$  by solving the problem (21), and use those in a classical sampling series to compute  $f$ . In practice, we consider a finite number of samples spread over some interval  $[J_1, J_2]$ , and we set  $M = \lfloor \frac{1}{2T}(J_1 + J_2) \rfloor$  to center the basis  $h(n, t)$  appropriately.

Once we have recovered the function  $f$ , we perform some elementary calculations with Fourier transforms to find that

$$P^+ f_N(t) = \sum_{n=-N}^N \tilde{c}_{n,N} \frac{1}{2} \text{sinc}\left(\frac{t - n - M}{2}\right) e^{\frac{\pi i}{2}(t - n + M)}$$

and

$$\frac{d}{dt} P^+ f_N(t) = \sum_{n=-N}^N \tilde{c}_{n,N} \frac{(i + \pi(t - n - M)) e^{\pi i(t - n + M)} - i}{2\pi(t - n - M)^2},$$

from which we can approximate  $\text{IF}_H f$ . Note that the Synchrosqueezing-based method discussed in Section 3 determines the IF components (as defined by  $\text{IF}_S$ ) of the function  $f$  directly, while the approach considered in this section treats the function  $f$  as a whole and determines its IF (given by  $\text{IF}_H$ ) after the signal itself has been recovered.

We finally make a few comments on the applicability of the framework discussed in this section. The assumption that  $f \in L^2$  can be weakened to  $f \in L^\infty$  in practice. Suppose  $B$  is a function such that  $\hat{B}$  is smooth,  $\hat{B}(0) = 1$  and  $\text{supp}(\hat{B}) \subset [-1, 1]$ . For  $\frac{1}{T} > 2b$ , any  $f \in L^\infty$  with  $\text{supp}(\hat{f}) \subset [-b, b]$  can be expressed as the sampling series

$$f(t) = \sum_{k=-\infty}^{\infty} f(Tk) \text{sinc}\left(\frac{t}{T} - k\right) B\left(\left(\frac{1}{T} - 2b\right)(t - k)\right),$$

which converges uniformly on compact sets [4]. If we restrict our attention to a fixed finite interval  $I$ , then  $f$  can be well approximated on  $I$  by taking a finite part of this series  $f_p \in L^2$ , which has  $\text{supp}(\hat{f}_p) \subset [-(\frac{1}{T} - b), (\frac{1}{T} - b)]$ . As long as  $f$  is oversampled, our reconstruction method will approximately recover  $f_p$ . In the next section, we will apply the least-squares method to AM-FM functions  $f$  of the type in Definition 3.2, which are generally not strictly bandlimited, but by considering Fourier series on a given finite interval  $I$ , such functions can be closely approximated on  $I$  by bandlimited  $L^\infty$  functions that have a sufficiently high bandwidth (see [14] for details). In practice, if our sampling interval  $T$  is greater than  $\sup_{k, t \in I} \text{PIF}(f, A_k, \phi_k)$ , we can recover  $f$  effectively.

## 5 Numerical Experiments and Applications

We use the algorithms discussed in Sections 3 and 4 on several test cases. We consider an AM-FM signal, a chirp signal, a bandlimited Bessel function, a Fourier harmonic contaminated by noise, an undersampled harmonic, a multi-component signal and finally, a signal with interlacing IIF elements. These are respectively shown in Figures 1-7 below. We compute the  $\text{IF}_S$  of these signals using STFT Synchrosqueezing and the  $\text{IF}_H$  using the bandlimited reconstruction method. For the  $\text{IF}_S$  computation, the Gaussian window function  $g(t) = e^{-0.1\pi t^2}$  and the parameters  $\alpha = 0.1$  and  $\gamma = 10^{-8}$  work well in practice, and we use these values unless stated otherwise.

In all of these examples, we use sampling times that are random perturbations of uniformly spaced times and have the form  $t_n = Tn + T'a_n$ , where  $T' < T$  and  $\{a_n\}$  is a fixed realization of a white noise process uniformly distributed in  $[0, 1]$ . For purposes of comparison, we also test most of these examples with uniform samples as well, i.e.  $T' = 0$ . In the figures below, the first two images are respectively  $\text{IF}_S f$  and  $\text{IF}_H f$  determined from uniform samples, while the two latter images are  $\text{IF}_S f$  and  $\text{IF}_H f$  for the general case of nonuniform samples.

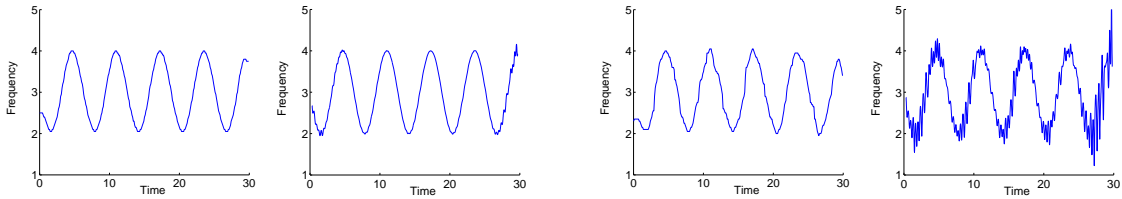


Figure 1: The AM-FM signal  $f(t) = (2 + \cos t) \cos(2\pi(3t + \cos t))$ ,  $t \in [0, 30]$ . The samples are taken at  $t_n = 0.1n + T'a_n$ ,  $T' = 0$  (left images) and  $T' = 0.08$  (right images). The IIF is  $3 - \sin t$ , and both methods produce results that are reasonably close to this.

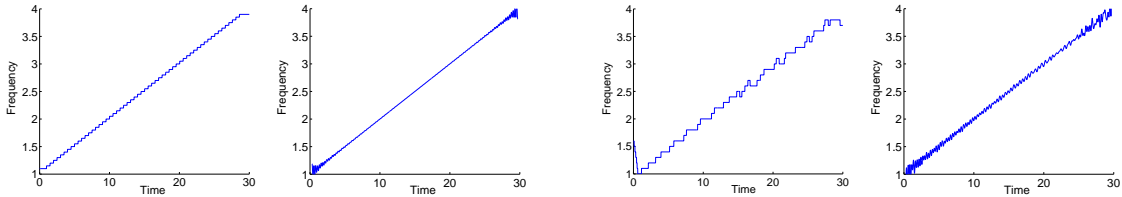


Figure 2: The chirp signal  $f(t) = \cos(2\pi(t + 0.05t^2))$ ,  $t \in [0, 30]$ , with samples taken at  $t_n = 0.1n + T'a_n$ ,  $T' = 0$  (left images) and  $T' = 0.08$  (right images). The IIF in this case is  $1 + 0.1t$ , and both methods produce results that are very close to this.

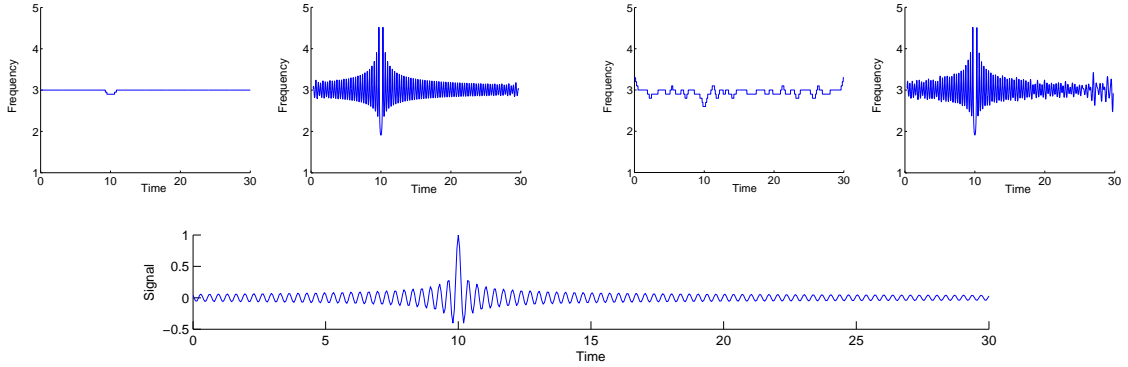


Figure 3: The bandlimited signal  $f(t) = J_0(6\pi(t - 10))$ ,  $t \in [0, 30]$ , where  $J_0$  is the Bessel function of order 0 (see [15]). The samples are taken at  $t_n = 0.1n + T'a_n$ ,  $T' = 0$  (left images) and  $T' = 0.08$  (right images). There is no way to determine the IIF in this case, but it can be shown that  $J_0(0) = 1$  and  $J_0(t) \approx \sqrt{\frac{2}{\pi|t|}} \cos(|t| - \frac{\pi}{4})$  when  $|t|$  is large, so we would expect the IF to be roughly the constant 3. The computed  $\text{IF}_S f$  agrees with our intuition here. On the other hand,  $\text{IF}_H f$  is highly oscillating, particularly around  $t = 10$ , which indicates that it is unable to clearly distinguish between the amplitude and frequency factors of  $f$ . We also show the graph of  $f$  itself at the bottom for clarity.

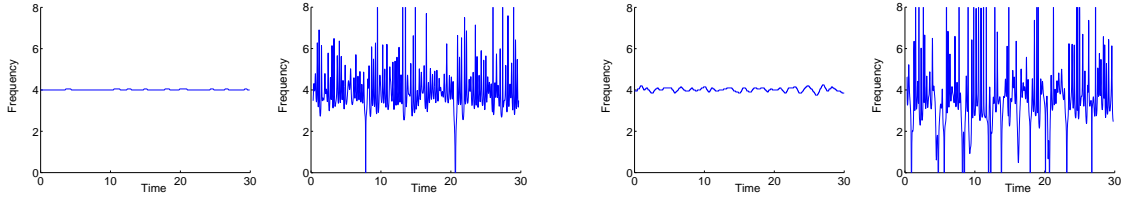


Figure 4: The signal  $f(t) = \cos(8\pi t) + N_t$ ,  $t \in [0, 30]$ , where  $N_t$  is a realization of Gaussian white noise with mean 0 and variance  $\sigma^2 = 0.4$ . The samples are taken at  $t_n = 0.1n + T'a_n$ ,  $T' = 0$  (left images) and  $T' = 0.08$  (right images). The computation of  $\text{IF}_S f$  is fairly robust to the noise, while that of  $\text{IF}_H f$  gives very poor results.

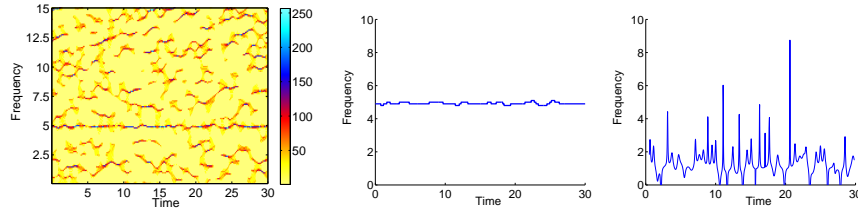


Figure 5: The signal  $f(t) = \cos(10\pi t)$ ,  $t \in [0, 30]$ , with samples taken at  $t_n = 0.25n + 0.2a_n$ . The IIF is the constant 5. Note that this signal is heavily undersampled, with a sampling rate of less than half its Nyquist rate. We take  $\gamma = 6$  for the STFT Synchrosqueezing computation, which produces a good result for  $\text{IF}_S f$  despite the low sampling rate, but the bandlimited reconstruction method cannot determine  $\text{IF}_H f$ . In this example, we also show the time-frequency plot of  $S^{\alpha, \gamma}$  (the first image) to illustrate how the IF curve appears in it, before we extract it out.

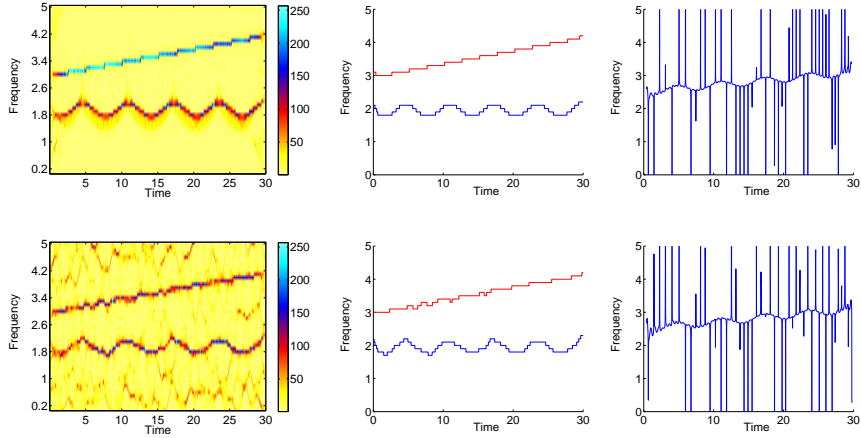


Figure 6: The two-component signal  $f(t) = \cos(2\pi(2t + 0.2 \cos t)) + \cos(2\pi(3t + 0.02t^2))$ ,  $t \in [0, 30]$ , with samples taken at  $t_n = 0.1n + T'a_n$ ,  $T' = 0$  (top images) and  $T' = 0.08$  (bottom images). We would like to recover both elements of the IIF set  $\{2 - 0.2 \sin t, 3 + 0.04t\}$ , and the  $\text{IF}_S$  calculation succeeds in doing this. In contrast, the  $\text{IF}_H$  concept cannot separate the components, instead roughly giving their average  $2.5 + 0.02t - 0.1 \sin t$ , and its computation also exhibits spurious singularities.

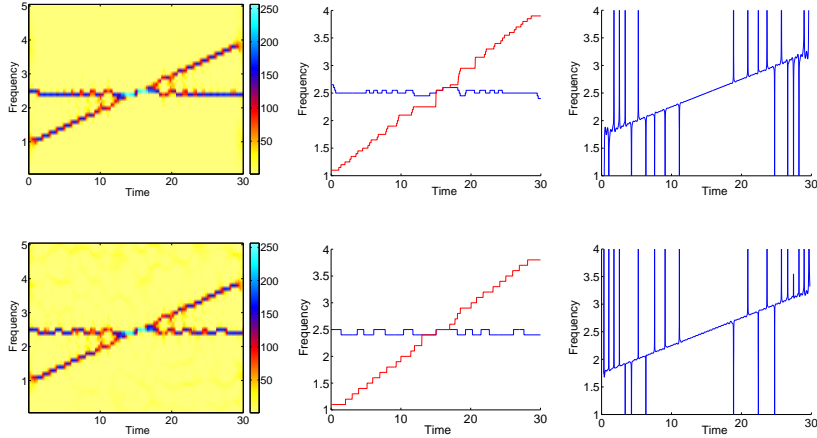


Figure 7: The signal  $f(t) = \cos(5\pi t) + \cos(2\pi(t + 0.05t^2))$ ,  $t \in [0, 30]$ , with samples taken at  $t_n = 0.1n + T'a_n$ ,  $T' = 0$  (top images) and  $T' = 0.08$  (bottom images). This example is similar to the previous one but the IIF curves cross each other. However, the plot of  $S^{\alpha,\gamma}$  shows a sharp separation between the two curves around the crossover point and can distinguish between them clearly.

The examples in Figures 3-7 show the advantages of the  $\text{IF}_S$  approach over the traditional  $\text{IF}_H$  concept. In Figure 5, the bandlimited reconstruction method fails to recover  $f$  accurately due to the low sampling rate, and this is reflected in the computation of  $\text{IF}_H f$ , but STFT Synchrosqueezing still manages a good result. This can be possibly explained by the fact that the Nyquist rate is essentially a concept for bandlimited signals and is only relevant in that context, whereas our STFT Synchrosqueezing theory is built around  $\mathcal{B}_{\epsilon,d}$  signals and only estimates their IIF, not the signals themselves. In Figures 4, 6 and 7, our sampling rate is high enough and the bandlimited reconstruction method can accurately determine  $f$  itself, but the subsequent calculation of  $\text{IF}_H f$  amplifies the effects of any noise or numerical roundoff errors. In contrast, we find that  $\text{IF}_S f$  is robust to such disturbances. We also note that determining a meaningful IF for the



type of signal in Figure 7 is often difficult [7] and such signals are certainly not in the class  $\mathcal{B}_{\epsilon,d}$ , but the result is nevertheless very good.

We now discuss a real-world problem in electrocardiography (ECG) to which our methods are applicable. In addition to describing the heart's electrical activity, the ECG signal contains information about a signal describing respiration. It is important in many clinical situations to be able to determine properties of this respiration signal from the ECG signal. For example, in an examination for tachycardia during sleeping, where only the ECG signal and no respiration signal is recorded, it allows for the detection and classification of sleep apnea. It is well known in the ECG field that the customary surface ECG signal is influenced by respiration, since inhalation and exhalation change the thoracic electrical impedance, which suggests that the respiration signal can be estimated from the ECG signal. The ECG-Derived Respiration (EDR) class of techniques [13], in development since the late 1980s, accomplish this and have proved to be a useful clinical tool. We now show that STFT Synchrosqueezing provides an alternative method to extract key information about the respiration signal from an ECG signal. We can find the instantaneous frequency profile of the respiration signal, which gives a more precise and adaptive description of respiration than many of the existing techniques.

In Figure 8, we are given the lead II ECG signal and the true respiration signal of a healthy 30 year old male, recorded over an 8 minute interval. The sampling rates of the ECG and respiration signals are respectively 512Hz and 64Hz. We take the R peaks (the sharp, tall spikes in the first image in Figure 8) of the ECG signal and use these samples to approximate the IF of the respiration signal, without using any knowledge of the actual respiration signal. We do not have samples of the respiration signal itself, but we can view the R peaks as samples of an envelope of the ECG signal, and based on the physiological facts discussed above, this envelope would be expected to have the same IF profile as the actual respiration signal. We apply the methods from Sections 3 and 4 to compute  $IF_S$  and  $IF_H$  from the R peaks, and use the actual, recorded respiration signal to compare the validity of our results. Let the ECG and true respiration signals be denoted by  $E(t)$  and  $R(t)$  respectively, where  $t \in [0, 480]$  seconds. There are 589 R peaks appearing at times  $t_k \in [0, 480]$ ,  $t_k < t_{k+1}$ ,  $1 \leq k \leq 589$ . For the calculation of  $IF_S$ , we use the impulse train-like function

$$\tilde{f}_{Rpeaks}(t) = \begin{cases} (t_k - t_{k-1})E(t) & \text{if } t = t_k \\ 0 & \text{otherwise} \end{cases} ,$$

and for  $IF_H$ , we simply use the samples  $\{E(t_k)\}$ . The results are shown in Figure 8 below. The third image in Figure 8 shows that the  $IF_S$  computed from  $\tilde{f}_{Rpeaks}$  is a good approximation to the  $IF_S$  of the true respiration signal  $R(t)$ . On the other hand, the  $IF_H$  determined from the R peaks in the fourth image has little in common with  $IF_H R(t)$ . In fact,  $IF_H R(t)$  is often negative and admits no obvious interpretation, unlike the  $IF_S$ . This is likely a result of the fact that ECG measurements usually contain large amounts of noise, which  $IF_H$  does not handle well, and many standard noise reduction techniques are not applicable here since they would smooth out the R peaks. In Figure 9, it can be seen that the spacing of respiration cycles in  $R(t)$  is reflected by  $IF_S$  of the R peaks; closer spacing corresponds to higher  $IF_S$  values, and wider spacing to lower  $IF_S$  values.

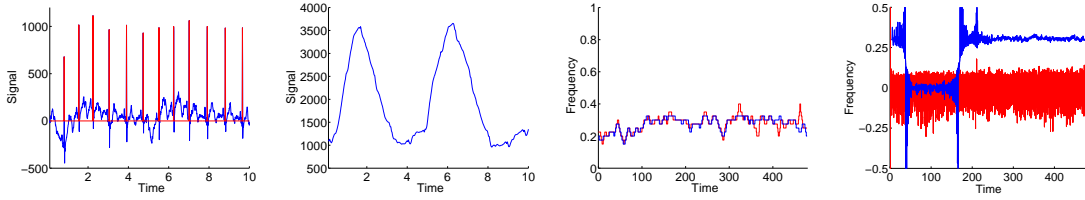


Figure 8: First Image: A 10-second part of the ECG signal. The R peaks are highlighted in red. Second Image: A 10-second part of the respiration signal. Third Image: The  $IF_S$  computed from  $\tilde{f}_{Rpeaks}$  (blue) and the  $IF_S$  of the actual respiration signal  $R(t)$  (red). Fourth Image: The  $IF_H$  computed from  $E(t_k)$  using bandlimited reconstruction (blue) and the  $IF_H$  of  $R(t)$  (red).

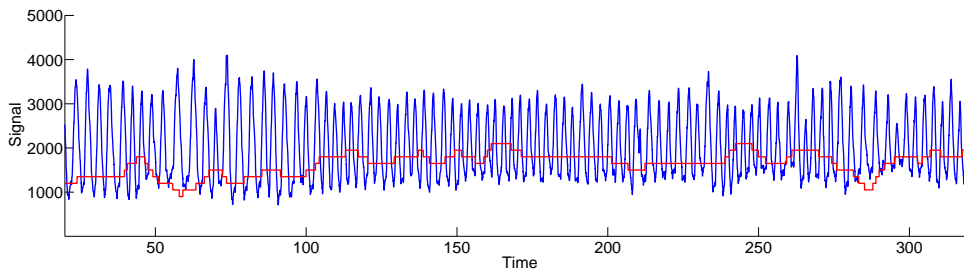


Figure 9: The first 300 seconds of  $R(t)$  (blue) with the  $IF_S$  estimated from  $\tilde{f}_{Rpeaks}$  (red) superimposed on top of the graph of  $R(t)$ .

*Acknowledgement.* The authors would like to thank Professor Ingrid Daubechies for many valuable discussions in the course of this work, and Dr. Ray F. Lee for assistance in collecting the respiration signal. H.-T. Wu also acknowledges discussions with Dr. Shu-Shya Hseu and Prof. Chung-Kang Peng. The authors acknowledge support by FHWA grant DTFH61-08-C-00028.

## References

- [1] A. ALDROUBI AND K. GRÖCHENIG, *Nonuniform sampling and reconstruction in shift-invariant spaces*, SIAM Review, 43 (2001), pp. 585–620.
- [2] F. AUGER, E. CHASSANDE-MOTTIN, AND P. FLANDRIN, *Time-frequency/time-scale reassignment*, in Wavelets and signal processing, Appl. Numer. Harmon. Anal., Birkhäuser Boston, Boston, MA, 2003, pp. 233–267.
- [3] T. BERKANT AND J. L. PATRICK, *Comments on the Interpretation of Instantaneous Frequency*, IEEE Sig. Proc. Letters, 4 (1997), pp. 123–125.
- [4] L. L. CAMPBELL, *Sampling Theorem for the Fourier Transform of a Distribution with Bounded Support*, SIAM J. of Appl. Math., 16 (1968).
- [5] I. DAUBECHIES, J. LU, AND H.-T. WU, *Synchrosqueezed Wavelet Transforms: an empirical mode decomposition-like tool*, Appl. Comp. Harmonic Anal., (2010).
- [6] I. DAUBECHIES AND S. MAES, *A nonlinear squeezing of the continuous wavelet transform based on auditory nerve models*, in Wavelets in Medicine and Biology, A. Aldroubi and M. Unser, eds., CRC Press, 1996, pp. 527–546.

- [7] N. DELPRAT, B. ESCUDIE, P. GUILLEMAIN, R. KRONLAND-MARTINET, P. TCHAMITCHIAN, AND B. TORRESANI, *Asymptotic wavelet and Gabor analysis: extraction of instantaneous frequencies*, IEEE Trans. Information Theory, 38 (1992), pp. 644–664.
- [8] R. J. DUFFIN AND A. C. SCHAEFFER, *A Class of Nonharmonic Fourier Series*, Trans. American Math. Soc., 72 (1952), pp. 341–366.
- [9] H. G. FEICHTINGER, K. GRÖCHENIG, AND T. STROHMER, *Efficient numerical methods in non-uniform sampling theory*, Numerische Math., 69 (1995), pp. 423–440.
- [10] K. GRÖCHENIG, *Irregular Sampling, Toeplitz Matrices and the Approximation of Entire Functions of Exponential Type*, Math. of Computation, 68 (1999), pp. 749–765.
- [11] N. E. HUANG, Z. WU, S. R. LONG, K. C. ARNOLD, X. CHEN, AND K. BLANK, *On Instantaneous Frequency*, Adv. in Adaptive Data Anal., 1 (2009), pp. 177–229.
- [12] F. MARVASTI, *Nonuniform Sampling: Theory and Practice*, Kluwer, New York, 2001.
- [13] G. B. MOODY, R. G. MARK, A. ZOCCOLA, AND S. MANTERO, *Derivation of respiratory signals from multi-lead ECGs*, Computers in Cardiology, (1985).
- [14] B. SCHOTTSTAEDT, *An Introduction to FM*, (2010). <https://ccrma.stanford.edu/software/snd/snd/fm.html>.
- [15] E. T. WHITTAKER AND G. N. WATSON, *A Course of Modern Analysis, Fourth Ed.*, Cambridge Math. Library, Cambridge U. Press, Cambridge, UK, 1927.